Available online at www.sciencedirect.com

SciVerse ScienceDirect

Ceramics International 39 (2013) 6299–6302

CERAMICS INTERNATIONAL

www.elsevier.com/locate/ceramint

Solid state reaction preparation and enhanced red luminescence of S-doped $La_2Mo_2O_9$:Pr^{3+} phosphors

Dandan Zhang[a], Shikao Shi[a,*], Ming Luo[a], Ji Zhou[b]

[a]College of Chemistry & Materials Science, Hebei Normal University, Shijiazhuang 050024, China
[b]State Key Laboratory of New Ceramics and Fine Processing, Tsinghua University, Beijing 100084, China

Received 6 December 2012; received in revised form 15 January 2013; accepted 16 January 2013
Available online 1 February 2013

Abstract

Red-light-emitting phosphors of $La_2Mo_2O_9$:Pr^{3+} and S-doped $La_2Mo_2O_9$:Pr^{3+} were prepared by high temperature solid state reaction. Under the excitation of 450 nm blue light, all samples produced a red emission peak at 650 nm corresponding to the characteristic transition of Pr^{3+} ($^3P_0 \rightarrow {}^3F_2$). The dependence of Pr^{3+} doping content (x) on the luminescent intensity was analyzed, and the optimal doping content of Pr^{3+} was $x=0.07$. After a small quantity of sulfur was introduced into the system, the luminescence intensity of phosphors was obviously enhanced. The reasons for the enhancement of luminescence are due to improved crystallization after S doping and the relatively large electronegativity difference between S and Mo. Additionally, the coincidence of the excitation wavelength with the emission of GaN chips may recommend this phosphor system as a potential candidate for use in white light-emitting diodes.

Keywords: A. Powders: solid state reaction; B. Spectroscopy; C. Optical properties; Phosphor

1. Introduction

Recently, white light-emitting diodes (LED) have been given great attention due to their evident merits over traditional incandescent and fluorescent lamps [1,2]. In general, a white LED is produced through a combination of a blue InGaN chip with commercial $Y_3Al_5O_{12}$:Ce^{3+} (YAG:Ce) yellow-emitting phosphor [3,4]. Unfortunately, the combination has disadvantages of low color-rendering index because of the lack of sufficient red content. In addition, some sulfide phosphors including Y_2O_2S:Eu^{3+} and (Ca,Sr)S:Eu^{2+} are commercially applied as red phosphors for white LEDs. However, they have inferior chemical stability [5,6]. Therefore, it is necessary to solve the deficiency by developing suitable red phosphors excited with blue light, which possess good chemical stability and high efficiency.

The $La_2Mo_2O_9$ compound has two phases, transforming between a low-temperature form (α-$La_2Mo_2O_9$) and a high-temperature form (β-$La_2Mo_2O_9$) [7]. The latter type has been investigated as an ion conductor, and exhibits a cubic structure [8–10]. Due to satisfactory chemical and thermodynamic stability, β-$La_2Mo_2O_9$ may be suitable as a host for phosphors. If it is used as a host material, some ions can be introduced to the La site and Mo site. This will contribute to the selection of appropriate ion doping compositions and lead to the luminescence enhancement in the system. Recently, our group prepared Eu^{3+} doped β-$La_2Mo_2O_9$ and observed an increase in the red emission intensity of Eu^{3+} by doping different additional ions [11].

As an attractive activator among rare earth ions, Pr^{3+} offers the possibility of simultaneous blue ($^3P_0 \rightarrow {}^3H_4$), green ($^3P_0 \rightarrow {}^3H_5$) and red ($^3P_0 \rightarrow {}^3F_2$) emission for laser action as well as infrared (IR) emission for optical amplification [12]. Since Diallo et al. [13] reported the red phosphor $CaTiO_3$:Pr^{3+}, the investigation of Pr^{3+}-activated luminescent materials has become more and more popular [14–17]. In this paper, Pr^{3+} activated β-$La_2Mo_2O_9$ phosphors were prepared by conventional

---

*Corresponding author. Tel./fax: +86 311 8078 7402.
E-mail addresses: ssk02@mails.tsinghua.edu.cn, shishikao@gmail.com (S. Shi).

0272-8842/$ - see front matter © 2013 Elsevier Ltd and Techna Group S.r.l. All rights reserved.
http://dx.doi.org/10.1016/j.ceramint.2013.01.052

solid state reaction. Under the excitation of blue light, the red-light emission of Pr^{3+} was observed and the optimum Pr^{3+}-doping concentration was determined. After a small quantity of S doping into the system, the luminescent intensity of the phosphors was greatly enhanced. This is a welcome improvement in terms of applications for the phosphor system in white LEDs.

2. Experimental

A series of phosphors $La_{2-x}Pr_xMo_2O_9$ ($x = 0.01$–0.10) and $La_{2-x}Pr_xMo_{2-y}S_yO_9$ ($x = 0.07$, $y = 0.01$–0.07) were prepared by solid state reaction. The starting materials contain La_2O_3 (99.95%), MoO_3 (99.9%), Pr_6O_{11} (99.9%) and $(NH_4)_2SO_4$ (A.R.). The stoichiometric mixtures were first ground thoroughly in an agate mortar, and then preheated in a muffle furnace at 550 °C for 3 h. After regrinding, the mixtures were heat-treated for another 3 h. Finally, the samples were cooled to room temperature for characterization.

The structure of the samples was indexed with a D8 ADVANCE/Germany Bruker X-ray diffractometer (XRD) with Cu Kα radiation ($\lambda = 1.5406$ Å) at 40 kV and 40 mA. The scan range (2θ) was collected from 20° to 50° stepping at 3°/min. To confirm the addition of S into the phosphor, the energy dispersive X-ray spectroscopy (EDS) of one sample was measured using a S-570 scanning electron microscope (SEM). The excitation and emission spectra were measured by using an F-4600 spectrofluorometer equipped with a Xe lamp as excitation source. To reduce the error, the luminescence intensity from samples was measured at least twice. All the measurements were performed at room temperature.

3. Results and discussion

3.1. Structure of the phosphor samples

The XRD patterns of $La_{1.93}Pr_{0.07}Mo_2O_9$ prepared at 800–900 °C and $La_{1.93}Pr_{0.07}Mo_{1.97}S_{0.03}O_9$ prepared at 900 °C are shown in Fig. 1. The predominant diffraction peaks for all $La_{1.93}Pr_{0.07}Mo_2O_9$ samples correspond to reflection (210) of β-$La_2Mo_2O_9$ phase at about 27.84° (2θ). When the sintering temperature is 800 and 850 °C, some side peaks near (210), (211) and (320) (labeled with * in Fig. 1) can be noticed, which derive from the splits of the cubic structure of (210), (211) and (320) respectively. In addition, there are three tiny diffraction peaks near 33.42°, 33.97° and 48.82° (labeled with # in Fig. 1). As the temperature is increased to 900 °C, the splits in reflection (210) and (320) almost vanish and the tiny diffraction peaks near 33.97° and 48.82° also disappear. In the meantime, the split in reflection (211) becomes weak and the predominant diffraction peak (210) is greatly enhanced. The result is almost in agreement with the reported data of β-$La_2Mo_2O_9$ (consistent with JCPDS card 23-1145), confirming the cubic phase stabilization at 900 °C. It has been reported that $La_2Mo_2O_9$ has two different polymorphs which are closely related with the formation temperature: high-temperature cubic β-$La_2Mo_2O_9$ and low-temperature monoclinic α-$La_2Mo_2O_9$ [7]. The diffraction peaks labeled with * and # should correspond to α-$La_2Mo_2O_9$ (800–850 °C). When the temperature is increased to 900 °C, most split peaks and the diffraction peaks labeled with * and # disappear or weaken. This implies that the host is mainly composed of β-$La_2Mo_2O_9$ at 900 °C despite the existence of a small percentage of α-$La_2Mo_2O_9$.

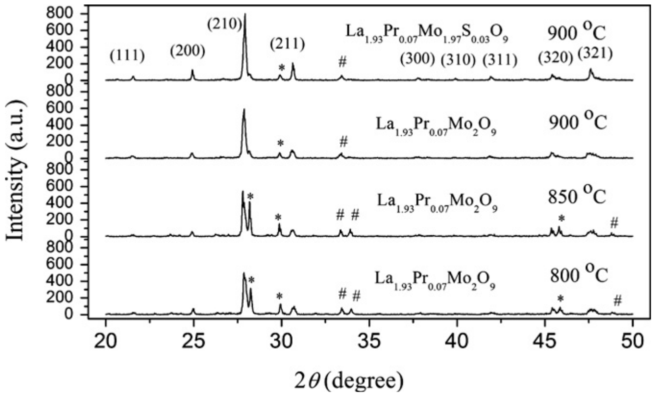

Fig. 1. XRD patterns of $La_{1.93}Pr_{0.07}Mo_2O_9$ and $La_{1.93}Pr_{0.07}Mo_{1.97}S_{0.03}O_9$ samples prepared at different temperatures.

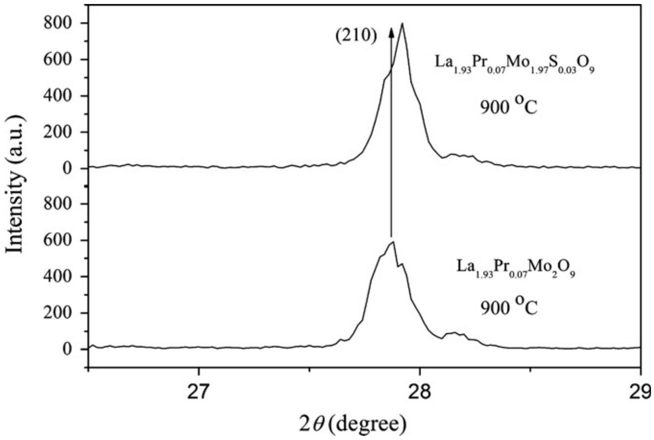

Fig. 2. Expanded version (from 26.5° to 29°) of XRD patterns of $La_{1.93}Pr_{0.07}Mo_2O_9$ and $La_{1.93}Pr_{0.07}Mo_{1.97}S_{0.03}O_9$ samples prepared at 900 °C.

The XRD pattern of $La_{1.93}Pr_{0.07}Mo_{1.97}S_{0.03}O_9$ prepared at 900 °C is also given in Fig. 1, which is very similar with that of $La_{1.93}Pr_{0.07}Mo_2O_9$ prepared at 900 °C. This means that assimilating a small amount of S into the host has little influence on the host structure. However, some changes can still be observed after S doping, as can be seen from Fig. 2. The predominant diffraction peak corresponding to reflection (210), located at 27.92°, undergoes a slight shift toward a higher diffraction angle. The reason is due to the relatively smaller ionic radius for S^{6+} (26 pm) as compared to Mo^{6+} (55 pm) in the same coordinate surroundings. After a small amount of S doping into the host, the cell parameter (*d* value) of the host is reduced. As a result, the diffraction angle (2θ) should be increased according to the empirical Bragg equation. In addition, the diffraction intensities (not only the predominant diffraction peak) of the sample are dramatically increased with the introduction of S, manifesting that the doping of S is quite beneficial in improving crystallization in the host.

3.2. Photoluminescence studies

The photoluminescence of all samples prepared at 900 °C was measured and their spectra are quite similar. Fig. 3 plots the excitation and emission spectra of $La_{1.93}Pr_{0.07}Mo_2O_9$ sample. Monitored with 650 nm, the excitation spectrum mainly consists of three excitation peaks, which are located at 450, 475, and 488 nm and correspond to $^3H_4 \rightarrow ^3P_2$, $^3H_4 \rightarrow ^3P_1$ and $^3H_4 \rightarrow ^3P_0$ transitions of Pr^{3+}, respectively. These peaks are coupled well with the emission of GaN chips. It is evident that the predominant excitation peak is at 450 nm, manifesting that the phosphor system can be effectively stimulated by 450 nm blue light. Under the excitation of 450 nm, the emission spectrum exhibits the characteristic red emission of Pr^{3+} ions, which are composed of three sharp lines belonging to the typical 4*f*–4*f* characteristic transitions of Pr^{3+}. The strongest emission line at 650 nm is ascribed to the $^3P_0 \rightarrow ^3F_2$ transition, while the other two weak emission lines around 620 nm and 604 nm are ascribed to the $^3P_0 \rightarrow ^3H_6$ and $^1D_2 \rightarrow ^3H_4$ transitions. The strong sharp emission peak at 650 nm should be of value in improving the color rendering index in white LEDs.

The emission intensity of the phosphor system is closely dependent upon the doping content of Pr (*x* value), and the emission intensity ($^3P_0 \rightarrow ^3F_2$ transition) dependence on *x* value are plotted in Fig. 4. It can be seen that the relative emission intensity of the $^3P_0 \rightarrow ^3F_2$ transition is strongly affected by the Pr^{3+} doping content. The emission intensity increases with the increase of *x* value up to 0.07, and then decreases with the further increase of *x* value owing to the concentration quenching effect. Therefore, $x=0.07$ is the optimal Pr^{3+} doping concentration for the formation of red phosphors.

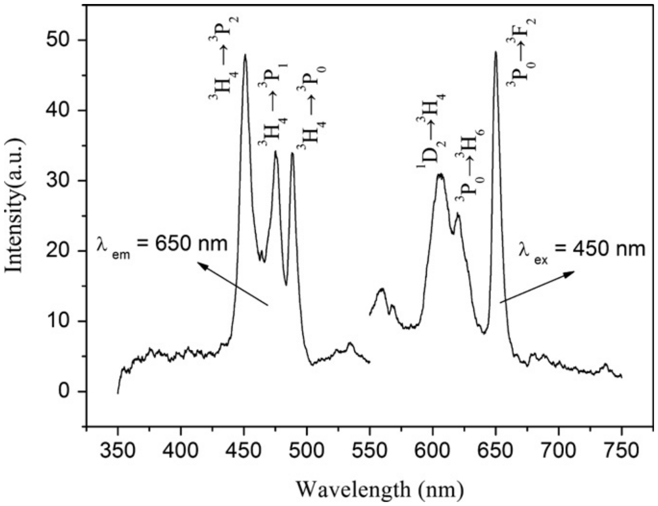

Fig. 3. Excitation ($\lambda_{em}=650$ nm) and emission spectra ($\lambda_{ex}=450$ nm) of $La_{1.93}Pr_{0.07}Mo_2O_9$ sample prepared at 900 °C.

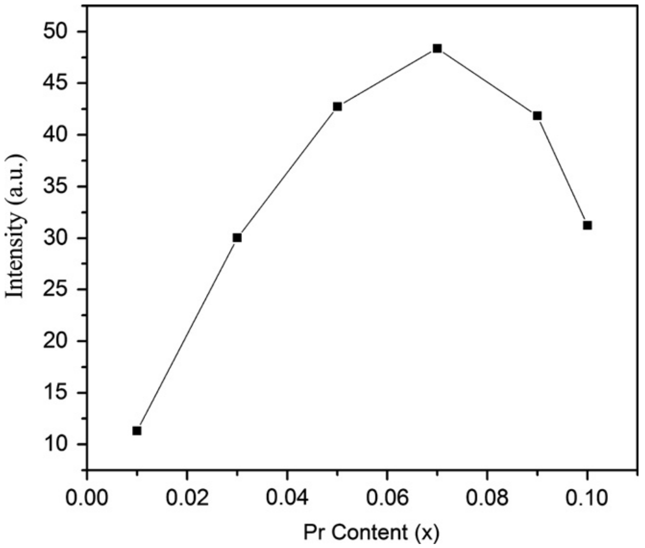

Fig. 4. Dependence of the emission intensity on Pr content (*x* value) in $La_{2-x}Pr_xMo_2O_9$ phosphor samples.

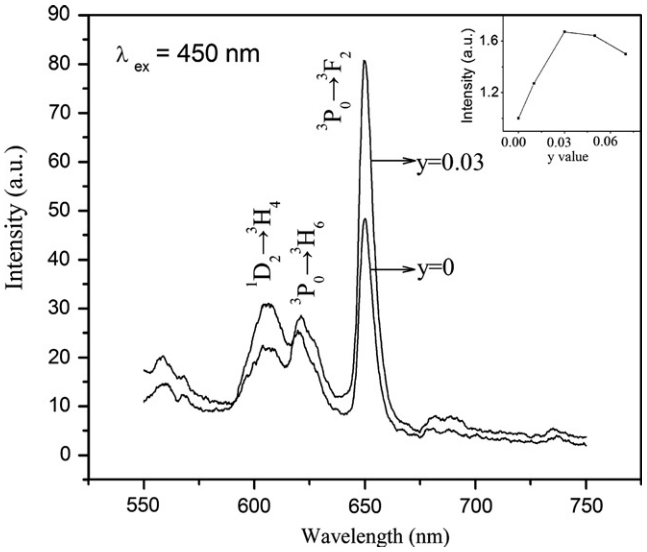

Fig. 5. Emission spectra ($\lambda_{ex}=450$ nm) of $La_{1.93}Pr_{0.07}Mo_{1.97}S_yO_9$ ($y=0$, 0.03) samples (inset is the dependence of relative luminescence intensity on S doping content (*y* value)).

The doping of a small amount of S into the phosphor system can influence the emission intensity of Pr^{3+}. Fig. 5 gives the emission spectra of $La_{1.93}Pr_{0.07}Mo_{1.97}S_yO_9$ ($y=0$, 0.03) and the Pr^{3+} relative intensity dependence on S doping content (*y* value). It is obvious that the $La_{1.93}Pr_{0.07}Mo_{1.97}S_{0.03}O_9$ ($y=0.03$) sample displays very strong luminescence intensity, which reaches more than 1.7-fold as compared with that of $La_{1.93}Pr_{0.07}Mo_2O_9$ sample.

In consequence, the S doping is advantageous to the enhancement of the luminescence intensity.

The enhanced luminescence of Pr^{3+}-activated $La_2Mo_2O_9$ phosphor system by S doping may be due to the following reasons. First, the improved crystallization after S doping is a positive factor to increase the emission intensity, which can be confirmed through XRD results. On the other hand, the large electronegativity difference between S (2.58) and Mo (2.16) can also influence the emission properties of the phosphors. The incorporation of S into the $La_2Mo_2O_9$ host can adjust the overlapping magnitude of the electronic cloud for Mo–O bond. A similar phenomenon has been observed in $NaEu(MoO_4)_2$ phosphors [18,19].

4. Conclusion

The Pr^{3+}-activated $La_2Mo_2O_9$ red-emitting phosphors have been prepared by conventional solid state reaction. The luminescence spectra of the samples indicate that all samples produce a red emission peak at 650 nm corresponding to the characteristic transition of Pr^{3+} ($^3P_0 \rightarrow {}^3F_2$) under the excitation of 450 nm blue light. The optimal doping concentration of Pr^{3+} is determined to be $x=0.07$. After a certain amount of S doping into the system, the red luminescence intensity of phosphors is further enhanced. The relative emission intensity of $La_{1.93}Pr_{0.07}Mo_{1.97}S_{0.03}O_9$ reaches more than 1.7-fold as compared with that of $La_{1.93}Pr_{0.07}Mo_2O_9$. Therefore, the phosphor system may be a good candidate for white LED applications.

Acknowledgments

This work was financially supported by the Natural Science Foundation of China (Grant no. 20971035), the Natural Science Foundation of Hebei Province (Grant nos. 08B012 and B2010000370), Science Foundation of Hebei Education Department (Grant no. 2009136) and the Research Foundation of Hebei Normal University (Grant no. L2008Z06).

References

[1] A. Bergh, G. Craford, A. Duggal, R. Haitz, The promise and challenge of solid-state lighting, Physics Today 54 (2001) 42–47.

[2] E.F. Schubert, J.K. Kim, Solid-state light sources getting smart, Science 308 (2005) 1274–1278.

[3] S. Nakamura, M. Seno, T. Mukai, High-power InGaN/GaN double-heterostructure violet light-emitting diodes, Applied Physics Letters 62 (1993) 2390–2392.

[4] B.Z. Yang, Z.P. Yang, Y.F. Liu, F.C. Lu, P.L. Li, Y.M. Yang, X. Li, Synthesis and photoluminescence properties of the high-brightness Eu^{3+}-doped $Sr_3Y(PO_4)_3$ red phosphors, Ceramics International 38 (2012) 4895–4900.

[5] J. Thirumalai, R. Jagannathan, D.C. Trivedi, $Y_2O_2S{:}Eu^{3+}$ nanocrystals, a strong quantum-confined luminescent system, Journal of Luminescence 126 (2007) 353–358.

[6] I.W. Park, J.H. Kim, J.S. Yoo, H.H. Shin, C.K. Kim, C.K. Choi, Longevity improvement of CaS:Eu phosphor using polymer binder coating for white LED application, Journal of the Electrochemical Society 155 (2008) J132–J135.

[7] F. Goutenoire, O. Isnard, R. Retoux, P. Lacorre, Crystal structure of $La_2Mo_2O_9$, a new fast oxide-ion conductor, Chemistry of Materials 12 (2000) 2575–2580.

[8] P. Lacorre, F. Goutenoire, O. Bohnke, R. Retoux, Y. Laligant, Designing fast oxide-ion conductors based on $La_2Mo_2O_9$, Nature 404 (2000) 856–858.

[9] S. Basu, P. Sujatha Devi, H.S. Maiti, A potential low-temperature oxide-ion conductor: $La_{2-x}Ba_xMo_2O_9$, Applied Physics Letters 85 (2004) 3486–3488.

[10] G. Corbel, E. Chevereau, S. Kodjikian, P. Lacorre, Topological metstastability and oxide ionic conduction in $La_{2-x}Eu_xMo_2O_9$, Inorganic Chemistry 46 (2007) 6395–6406.

[11] H.L. Gong, S.K. Shi, J. Zhou, Enhanced red luminescence of Eu^{3+} and R^{3+}-doped $La_2Mo_2O_9$ phosphors under blue light excitation, Current Applied Physics 11 (2011) 551–554.

[12] B. Grobelna, P. Bojarski, B. Kuklinski, A.A. Kubicki, A. Synak, Optical properties and luminescence kinetics of $Ln_{1.9}Pr_{0.1}(WO_4)_3$ (where Ln = Gd, La) immobilized in silica xerogel, Optical Materials 34 (2011) 103–108.

[13] P.T. Diallo, P. Boutinaud, R. Mahiou, J.C. Cousseins, Red luminescence in Pr^{3+}-doped calcium titanates, Physica Status Solidi A 160 (1997) 255–263.

[14] T. Kyomen, R. Sakamoto, N. Sakamoto, S. Kunugi, M. Itoh, Photoluminescence properties of Pr-doped (Ca, Sr, Ba) TiO_3, Chemistry of Materials 17 (2005) 3200–3204.

[15] X.Y. Yang, J. Liu, H. Yang, X.B. Yu, Y.Z. Guo, Y.Q. Zhou, J.Y. Liu, Synthesis and characterization of new red phosphors for white LED applications, Journal of Materials Chemistry 19 (2009) 3771–3774.

[16] W. Liang, Y.H. Wang, Energy transfer between Pr^{3+} and Mn^{2+} in $K_2YZr(PO_4)_3$:Pr, Mn phosphor, Materials Chemistry and Physics 127 (2011) 170–173.

[17] A. Lecointre, A. Bessiere, A.J.J. Bos, P. Dorenbos, B. Viana, S. Jacquart, Designing a red persistent luminescence phosphor: the example of $YPO_4{:}Pr^{3+}$, Ln^{3+} (Ln = Nd, Er, Ho, Dy), Journal of Physical Chemistry C 115 (2011) 4217–4227.

[18] Z.L. Wang, H.B. Liang, J. Wang, M.L. Gong, Q. Su, A novel red phosphor for near UV InGaN light-emitting diode and its luminescent properties, Materials Research Bulletin 43 (2008) 907–911.

[19] Y. Zhang, S.K. Shi, J. Gao, J. Zhou, Effects of ${SO_4}^{2-}$ or ${SO_3}^{2-}$ doping on the photoluminescence of $NaEu(MoO_4)_2$ nanophosphors for light-emitting diodes, Journal of Nanoscience and Nanotechnology 10 (2010) 2156–2160.